

Uncertainty in Measurements of Velocity and Concentration around a Building

Hideyuki Tanaka^a, Ryuichiro Yoshie^a, Cheng-Hu HU^a

^aTokyo Polytechnic University, 1583, Iiyama, Atsugi, Kanagawa, Japan

ABSTRACT: As with the progress of computing capacity in recent years, there have been many CFD studies concerned with the wind environment and the pollutant diffusion in urban areas. Currently, Steady solutions with RANS models (Steady RANS) are commonly used for this type of studies. However, CFD simulations with Steady RANS have some drawbacks that the reattachment length and pollutant gas concentration are overestimated behind the building, because they cannot reproduce periodic vortex shedding in the weak wind region behind the buildings. Therefore, applying the Steady RANS may be unsatisfactory for predicting pollutant diffusion and ventilation in the weak wind region behind the buildings. In this paper, we aim to provide adaptive experimental data required to verify the accuracy of numerical simulation. In order to show the reliability of experimental data, we evaluated the uncertainty of measurements for wind velocity and concentration, and verified the method for management of accuracy.

KEYWORDS: Wind tunnel test, Uncertainty of measurement, Pollutant diffusion, Wind velocity around a building

1 INTRODUCTION

CFD is expected as an effective means to predict and evaluate the wind environment and the pollutant diffusion in urban areas. Currently, Steady solutions with RANS models (Steady RANS) are commonly used for this type of studies. However, CFD simulations with Steady RANS have some drawbacks, where the reattachment length and pollutant gas concentration are overestimated behind the building, as they cannot reproduce periodic vortex shedding in the wake flows of a building. Therefore, applying the Steady RANS may be unsatisfactory for predicting pollutant diffusion and ventilation in the weak wind region behind the buildings. This problem may be solved by using LES, DES, or Unsteady RANS which can reproduce periodic vortex shedding in that region.

In this study, we aim to provide adaptive experimental data required to verify the accuracy of numerical simulation. Therefore, we applied the method for uncertainty of measurements. For this paper, we measured wind velocity and concentration around a building model simultaneously in a boundary layer wind tunnel.

2 EXPERIMENTAL SETUP

A square cylinder (100(x)×100(y)× 200(z)mm) was set on the wind tunnel floor and the approaching flow was modeled with a power-law profile with an exponent of $\alpha = 1/4$ (Figure 1). Tracer gas (C_2H_4) was released from a hole ($\varphi=2mm$) on the floor behind the square cylinder. The tracer gas flow was 0.35 l/min. Wind velocity components $\langle u_i \rangle + u_i'$ were measured by a split film probe (SFP) and the fluctuating concentration of tracer gas $\langle c \rangle + c'$ was measured by a fast response flame ionization detector (FID).

The accuracy of SFP was checked by measuring the wind velocity components for the angle of approaching wind θ from 0° to 180° (Figure 2).

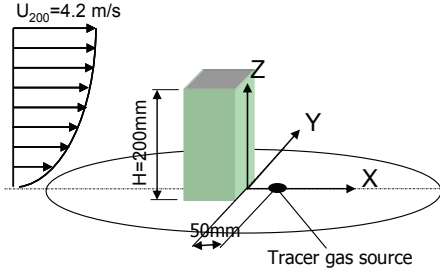


Figure 1. Object flow situation and Coordinate system

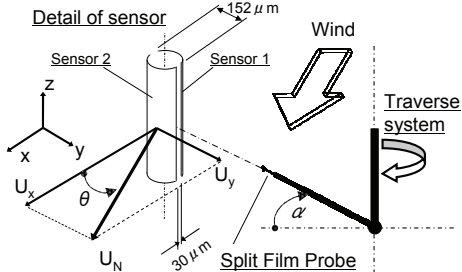


Figure 2. Detail of Split film probe (SFP)

3 DEFINITION AND EVALUATION OF UNCERTAINTY

According to ISO GUM [1], Uncertainty of measurements is defined as “Parameter, associated with the result of a measurement that characterizes the dispersion of the values that could reasonably be attributed to the measurand.” The expression method of the uncertainty is shown as follows. An estimate of measurand denoted by ζ , is a result of measurements given by

$$\zeta = f(\xi_1, \xi_2, \dots, \xi_N) \quad (1)$$

Where, $\xi_1, \xi_2, \dots, \xi_N$ are input estimates for the values of the N input quantities. The combined standard uncertainty $u_c(\zeta)$ of the measurement result ζ arises from the standard uncertainty $u(\xi_i)$ of the input estimates ξ_i . It is shown by equation (2).

$$u_c(\zeta) = \sqrt{\sum_{i=1}^N \left(\frac{\partial f}{\partial \xi_i} u(\xi_i) \right)^2} \quad (2)$$

The components of uncertainty $u(\xi_i)$ are categorized as Type A or Type B according to the method used to evaluate them. Type A evaluation is a method of evaluation for uncertainty by statistical analysis of a series of observations. In this method, the standard uncertainty $u(\xi_i)$ is estimated by standard deviation of mean by equation (3), where $s(\xi_i)$ is the standard deviation of ξ_i , n is degree of freedom. Type B evaluation is a method other than statistical analysis.

$$u(\xi_i) = \sqrt{\frac{s^2(\xi_i)}{n}} \quad (3)$$

In this experiment, a coverage factor k was calculated so that an interval having a level of confidence of approximately 95% could include a true value. And, we calculated the measurand Z by equation (4). Where, $U(\zeta)$ is an expanded uncertainty, which is defined by equation (5).

$$Z = \zeta \pm U(\zeta) \quad (4)$$

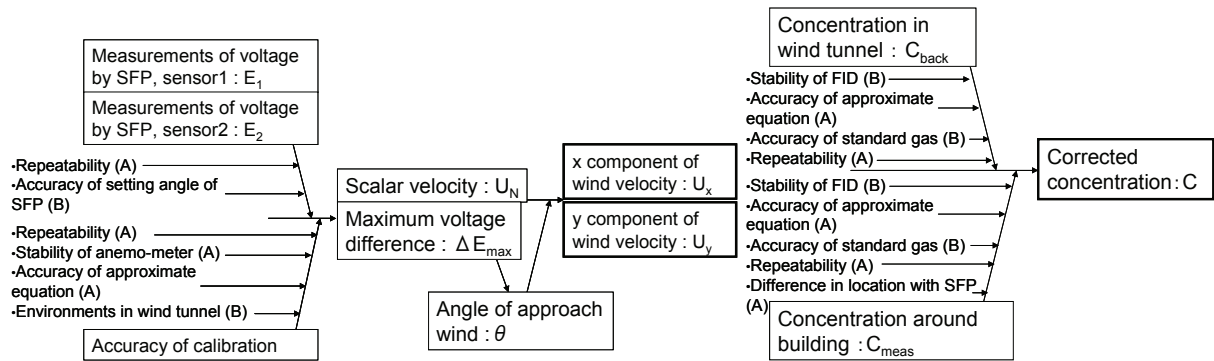
$$U(\zeta) = k u_c(\zeta) \quad (5)$$

In this experiment, there are some sources of uncertainty of measurement as shown in Figure 3. The results of uncertainty evaluation in preliminary experiment showed that the key factor was the setting angle of SFP. Therefore, we accurately adjusted this angle in this experiment.

4 EXPERIMENTAL RESULTS

4.1 Accuracy of Split film probe

The measurements by SFP and extended uncertainty $U(\zeta)$ for the cases of setting angle $\alpha = 0^\circ$ and 90° are shown in Table 1 and 2. And, in Figure 4, the scalar velocity U_N measured by SFP is



(a) Wind velocity measurement (Figure is an extracted part)

Figure 3. Sources of uncertainty of measurement (Inside of () is evaluation type)

compared with a calibration velocity U_{Nc} measured by Pitot tube. Measurements are good agreement with calibration velocity from Figure 4. These relative extended uncertainty ($=U(\zeta)/|\zeta|$) are about 3% in both of the tables.

In Figure 5, the angle of approaching wind θ measured by SFP is compared with the setting angle of SFP α . For the case of $30^\circ \leq \alpha \leq 150^\circ$, the measurements θ and the setting angle α are in good agreement. In the other angle range, the measurements θ have larger error of about 10° . However, in the case of larger error, the setting angle of SFP α is within the confidence level of 95% of measurand θ . For example, Table 1 show that $\alpha=0^\circ$ is included in $\theta = 7.593^\circ \pm 8.769^\circ$.

Figure 6 shows the components of wind velocity calculated by U_N and θ . The measurements of y components have larger error in the angle range of $\alpha \leq 30^\circ$ and $150^\circ \leq \alpha$. But for the measurements of x components, the relative extended uncertainties are as small as about 4% in all cases. Therefore, in this experiment the SFP was controlled so that it has an angle of approaching wind between 30° and 150° .

Table1 Uncertainty evaluation of measurements ($\alpha=0^\circ$)

Z	ζ	$U(\zeta)$	k
Scalar velocity : U_N (m/s)	4.041	± 0.074	2.00
Angle of approaching wind : θ (deg.)	7.593	± 8.769	2.13
x component of wind vel. : $U_x = \langle u \rangle$ (m/s)	4.006	± 0.175	2.08
y component of wind vel. : $U_y = \langle v \rangle$ (m/s)	0.534	± 0.559	2.13

Table2 Uncertainty evaluation of measurements ($\alpha=90^\circ$)

Z	ζ	$U(\zeta)$	k
Scalar velocity : U_N (m/s)	4.039	± 0.125	1.97
Angle of approaching wind : θ (deg.)	90.218	± 0.833	1.97
x component of wind vel. : $U_x = \langle u \rangle$ (m/s)	0.015	± 0.061	1.97
y component of wind vel. : $U_y = \langle v \rangle$ (m/s)	4.039	± 0.105	1.99

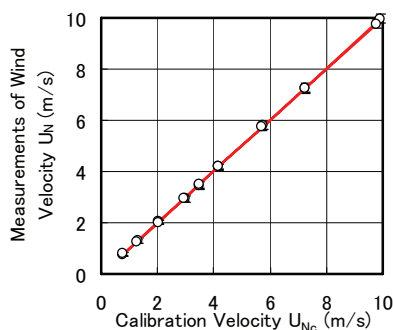


Figure4 Measurements of scalar velocity

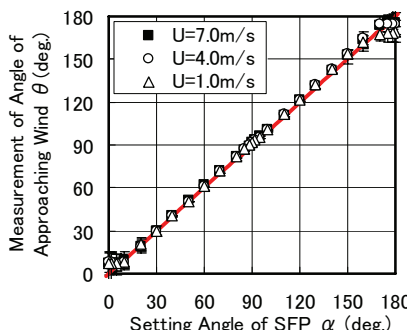


Figure5 Measurements of angle of approaching wind

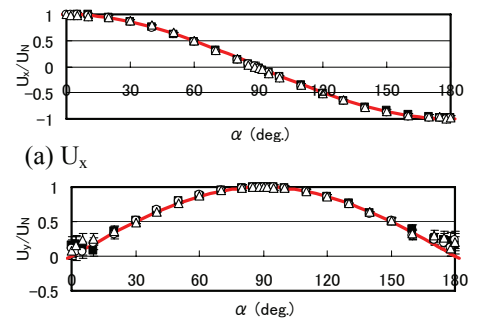


Figure 6 Components of wind velocity

4.2 Wind velocity and concentration diffusion around a building

The vertical profiles of mean wind velocity $\langle u \rangle$ are shown in Figure 7. Their relative extended uncertainty was 10% or less. And, reattachment length on the roof X_r and that behind the building X_f were $X_r/H=0.266 \pm 0.021$ and $X_f/H=0.686 \pm 0.064$.

The vertical profiles of turbulence intensities of concentration $\langle c' \rangle$ are shown in Figure 8. At the measuring locations by the side of building from the hole where the tracer gas is released, the extended uncertainty of $\langle c' \rangle$ showed the large value than other locations. The key source of uncertainty was due to the intermittency of peak concentration. And, the vertical profiles of concentration flux $\langle u'c' \rangle$ in Figure 9 showed the negative value at the left side of the hole, whereas positive value at the right side of the hole, which is consistent with what we had expected. On the other hand, $\langle w'c' \rangle$ in Figure 10 showed the positive value on all measuring locations.

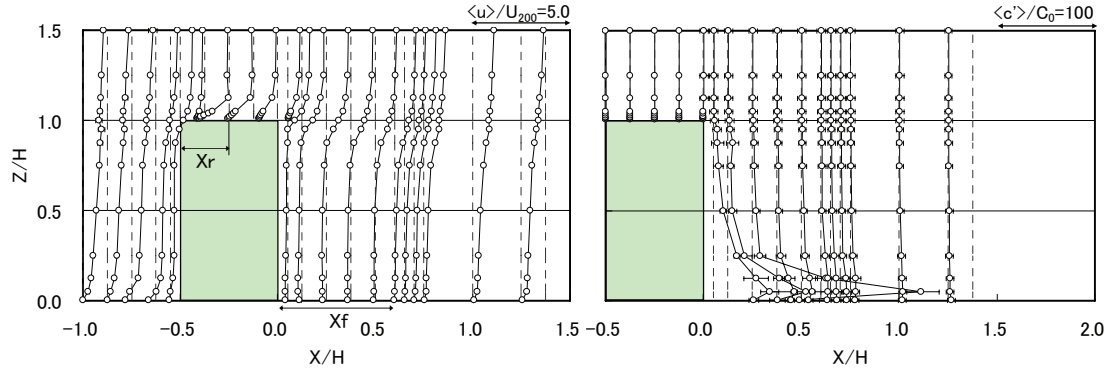


Figure 7 Mean wind velocity $\langle u \rangle$

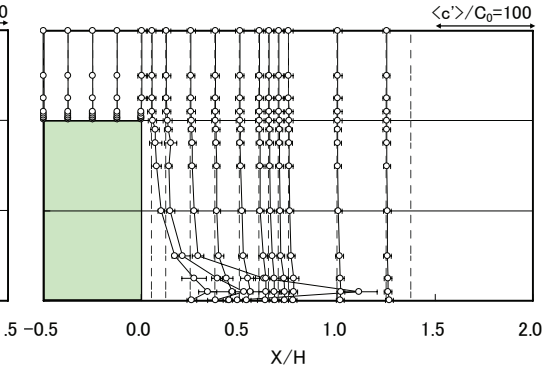


Figure 8 Turbulence intensity of concentration $\langle c' \rangle$

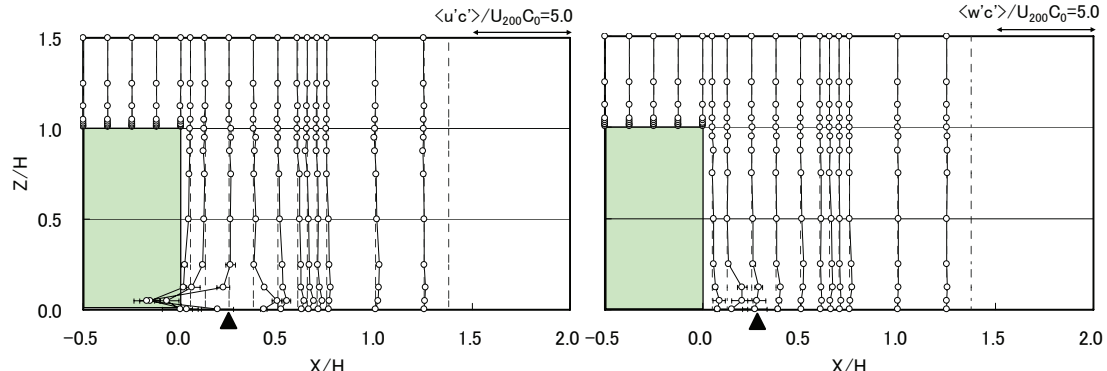


Figure 9 Concentration flux $\langle u'c' \rangle$

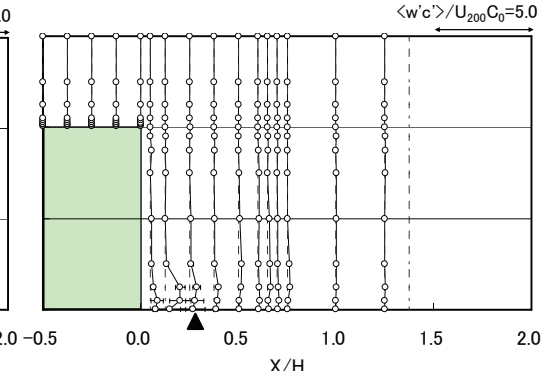


Figure 10 Concentration flux $\langle w'c' \rangle$

5 CONCLUSIONS

- 1) In order to obtain adaptive experimental data by split film probe, split film probe has to be set as much as possible so that it has an angle to the approaching wind between 30° and 150° .
- 2) The relative extended uncertainty of mean value of measurements is less than 10% for this experiment.
- 3) The intermittent peak concentration has influence on measured data.

In the future, we are going to use the result of this experiment to verify unsteady CFD models

6 ACKNOWLEDGEMENT

This study was partially funded by the Ministry of Education, Culture, Sports, Science and Technology, Japan, through the 21st Century Center of Excellence Program of Tokyo Polytechnic University.

7 REFERENCES

1 ISO, Guide to the Expression of Uncertainty in Measurement, 1993